

Inclusive Production of Electrons and Muons in Multihadronic Events at PETRA

CELLO Collaboration

H.J. Behrend, H. Fenner, M.-J. Schachter¹, V. Schröder, H. Sindt

Deutsches Electronen-Synchrotron, DESY, D-2000 Hamburg, Federal Republic of Germany

G. D'Agostini, W.-D. Apel, J. Engler, G. Flügge, D.C. Fries, W. Fues, K. Gamberinger,
G. Hopp, H. Küster, H. Müller, H. Randoll, G. Schmidt, H. Schneider

Kernforschungszentrum Karlsruhe and Universität Karlsruhe, D-7500 Karlsruhe, Federal Republic of Germany

W. de Boer, G. Buschhorn, G. Grindhammer, P. Grosse-Wiesmann, B. Gunderson, C. Kiesling, R. Kotthaus,
U. Kruse², H. Lierl, D. Lüers, H. Oberlack, P. Schacht

Max-Planck-Institut für Physik und Astrophysik, D-8000 München, Federal Republic of Germany

P. Colas, A. Cordier, M. Davier, D. Fournier, J.F. Grivaz, J. Haissinski, V. Journé,
F. Laplanche, U. Mallik, J.-J. Veillet

Laboratoire de l'Accélérateur Linéaire, F-91405 Orsay, France

J.H. Field³, R. George, M. Goldberg, B. Grossetête, O. Hamon, F. Kapusta, F. Kovacs,
G. London, L. Poggioli, M. Rivoal

Laboratoire de la Physique Nucléaire et Hautes Energies, Université de Paris, F-75230 Paris, France

R. Aleksan, J. Bouchez, G. Carnesecchi, G. Cozzika, Y. Ducros, A. Gaidot, Y. Lavagne,
J. Pamela, J.P. Pansart, F. Pierre

Centre d'Etudes Nucléaires, Saclay, F-91190 Gif-sur-Yvette, France

Received 6 June 1983

Abstract. The production of prompt leptons at PETRA has been measured for c.m. energies of 14, 22 and 34 GeV. The rate of prompt electrons and muons is presented, including a determination of the semileptonic branching ratio of the c and b quarks. We obtain

$$B(c \rightarrow \mu \nu X) = 12.3 \pm 2.9 (\text{stat.}) \pm 3.9 (\text{syst.}) \%,$$

$$B(b \rightarrow \mu \nu X) = 8.8 \pm 3.4 (\text{stat.}) \pm 3.5 (\text{syst.}) \%,$$

$$B(b \rightarrow e \nu X) = 14.1 \pm 5.8 (\text{stat.}) \pm 3.0 (\text{syst.}) \%.$$

Systematic effects due to changes in fragmentation and other model parameters have been studied.

I. Introduction

The e^+e^- annihilation into hadrons at PETRA energies is well described by assuming the pair production of u, d, s, c and b quarks and gluon bremsstrahlung. Pair production of t -quarks is excluded up to a center of mass (c.m.) energy of $W \approx 39$ GeV. Since weak decays of the hadrons containing light quarks (u, d, s) have guided the understanding of electroweak interactions, it is of great interest to explore the weak decays of hadrons containing heavy quarks (c, b). Assuming standard mixing angles, in the Kobayashi-Maskawa model [1] bottom is expected to decay predominantly into charm, and charm to strangeness.

The hadrons containing a b quark are expected to decay with a branching ratio of 11–17% both to $\mu \nu X$ and to $e \nu X$ [2] which agrees with recent

¹ Now at SCS, Hamburg, Germany

² Now at University of Illinois, Urbana, USA

³ On leave of absence from DESY, Hamburg, Germany

measurements [3]. In most cases, there should be one charmed hadron in X . The charmed hadrons have semileptonic branching ratios of the same magnitude [4].

The leptons resulting from the semileptonic decay of bottom hadrons are expected to dominate the region of transverse momentum larger than 1.0 GeV/c with respect to the jet axis. This feature combined with a more spherical event shape is used in the selection of hadronic $b\bar{b}(g)$ events.

The search for inclusive leptons in hadronic events provides therefore an indirect study of heavy quark production. From the inclusive lepton yield we obtain the fraction of "prompt" leptons, which result only from semileptonic b - or c -decays, including the cascade decay $b \rightarrow c \rightarrow l\nu X$ by subtracting all trivial lepton sources as π/K -decay, γ -conversion etc. The prompt lepton signals yield then with suitable additional cuts a measurement of the semileptonic branching ratios of heavy quarks.

A selection of events containing mostly $b\bar{b}(g)$ allows a measurement of the charge angular asymmetry predicted in the Weinberg-Salam model [7].

The final state hadrons result from the fragmentation of the original quarks. This fragmentation process is poorly known, and models with several free parameters are used to describe it. The measurement of the rate and spectra of inclusive leptons could thus help to understand better the fragmentation functions of heavy quarks. The model dependence of the determination of the semileptonic branching ratios has carefully been studied by comparing the data with the Hoyer et al. [5] and Lund [6] MC event generators. For both models branching ratios of

$$\text{Br}(c \rightarrow l\nu X) = 9 \pm 2\% \quad \text{and} \quad \text{Br}(b \rightarrow l\nu X) = 12 \pm 2\%$$

have been used.

II. Detector Description and Data Selection

The data were taken with the CELLO detector [8] at PETRA at average c.m. energies of $W=14, 22$ and 34 GeV. The corresponding integrated luminosities are 1.2 pb^{-1} , 2.5 pb^{-1} and 7.9 pb^{-1} .

Charged particles were measured in cylindrical drift and proportional chambers in a 1.3 T magnetic field yielding a momentum resolution of $\sigma(P)/P = 2\% \cdot P \cdot \sin\theta$ (P in GeV) over 92% of the solid angle of 4π .

For neutral particle reconstruction and electron identification we use the barrel part of a fine grain lead liquid argon calorimeter which has a solid angle acceptance of 86% of 4π . Each of 16 calori-

meter modules samples the energy deposited by particles in the liquid argon 17 times in depth. The energy is collected on lead strips of three different orientations up to a maximum of 21 radiation lengths (X_0). For each particle it is combined into 6 energy clusters in depth. The trajectory and energy of a particle is then reconstructed from up to 6 energy and position measurements. We obtain an energy resolution of $\sigma(E)/E = 13\%/\sqrt{E}$ (E in GeV) and an angular resolution of 4 mrad.

The muon detector covers 92% of 4π and consists of one layer of planar wire chambers detecting particles penetrating a hadron filter formed by the liquid argon calorimeter and 80 cm of iron. The minimal filter thickness is equivalent to 5.5 interaction lengths. Each chamber allows the reconstruction of space points using one layer of anode wires and two layers of tilted cathode strips. The spatial resolution of these chambers is of the order of 6 mm which matches the uncertainty due to the multiple scattering of muons in the hadron filter.

The trigger for the multihadronic final state and the event selection criteria have been described previously [9]. The most relevant data selection requirements were:

- (a) more than 4 reconstructed charged particles
- (b) fraction of total "visible energy" in charged particles $\sum E_i/W > 0.24$
- (c) event axis (thrust) in a polar angle range of $|\cos\theta| < 0.84$.

These cuts remove two-photon events very efficiently. The residual background from cosmic rays, beam-gas- and Bhabha-events has been removed by visual scan. The corresponding numbers of multihadronic events are then 2,100, 1,600 and 2,400 respectively at the three energies. These events were then studied for the presence of leptons.

III. Prompt Electrons

a) Electron Identification

To identify electrons all tracks measured in the inner detector have been extrapolated to the liquid argon calorimeter. In order to avoid regions with a rapid variation of the acceptance, we reduce the solid angle covered with each calorimeter module by a typically 30 mrad wide band at the edges. This leaves 74% of the solid angle. Two different strategies for electron identification were followed. Both methods employ the longitudinal energy deposition in the liquid argon calorimeter. The first method (I) tests the maximum of the lateral shower distribution in the individual fine sampling layers of given orientation. The second one (II) uses the development of

the entire shower as given by the energy clusters in depth from the reconstruction. Both methods require that the energy E deposited in the liquid argon calorimeter matches the momentum p as measured in the central detector. This cut is parameterized depending on momentum and demands typically $p/E < 1.6$ yielding 95% efficiency.

In method I we consider only the energy deposit on those channels that are within ± 1 channel widths on the particle trajectory, and select within this band the channel with the maximum energy deposit. We restrict the region used in depth to the second and third layer of the liquid argon calorimeter, extending from 1 to $5X_0$. With 3 orientations per layer we thus obtain 6 independent fractional energy measurements per particle. In addition, for particles below 3 GeV we demand no energy deposit in the last layer ($> 16X_0$). The individual cut-off parameters have been optimized with respect to π/e -separation by comparison with detailed MC simulations and test data. To do so, we finally used a momentum dependent parameterization of these cut-off parameters as obtained from the MC studies.

Method II tests the relative energy deposit of the particles in each of the 6 layers of the calorimeter as found after reconstruction. To perform this test we used MC generated electrons in a wide range of angle and momentum to obtain their relative energy deposit in each layer as well as the correlations between different layers. The longitudinal energy distribution of the reconstructed shower is then compared with the MC expectation using an angle and energy dependent parameterization.

With both methods we get electron efficiencies of 70% in the momentum range from 1 to 6 GeV with a pion misidentification probability of 2×10^{-3} as determined for isolated tracks from test measurements and MC studies.

In a multihadronic event we are faced with additional complications. The high density of both electromagnetic and hadronic interactions of particles in the liquid argon calorimeter may lead to a substantial overlap between clusters of deposited charge and thus worsen the energy resolution of the electron candidate. In addition, charged pions which are accompanied by nearby photons may fake electrons. Furthermore in this case the angular resolution of tracks reconstructed in the central detector is somewhat worse, yielding larger errors for the extrapolation to the liquid argon calorimeter. Thus the electron efficiency is reduced to typically 60%, and the pion misidentification probability is increased to 3×10^{-3} as studied in MC events.

In the following, results from method I are presented.

For all relevant processes MC generated events were propagated through the detector according to a detailed simulation of the CELLO detector. The simulation in the liquid argon calorimeter is based on the EGS-code [10] for the electromagnetic part and on the HETC-code [11] for the hadronic part. Explicit use of this simulation was made in a previous analysis [12] and detailed comparisons may be found there. Finally the MC data were then transformed into the original raw data structure and subsequently processed through the data reduction and analysis chain with the same cuts and constants as the real data.

b) Event Simulation and Background Subtraction

For the generation of multihadronic annihilation events we employed the Hoyer model [5] using Feynman-Field fragmentation [13]. The most important parameters of the model were tuned by detailed comparison with existing data.*

We investigated the influence of different fragmentation models on the results which will be discussed in detail in Chap. V.

Leptons from semileptonic decays of heavy quarks show a significantly different transverse momentum (p_{\perp})-distribution with respect to the thrust axis of the event than leptons from other sources. While most of the leptons produced in $u\bar{u}$, $d\bar{d}$, $s\bar{s}$ and $c\bar{c}$ pairs are expected to have rather small transverse momenta, $b\bar{b}$ events should dominate the p_{\perp} region typically above 1.0 GeV/c. Gluon emission and initial state radiation reduce the difference, but leave the separation still valid.

To reduce the background due to π -misidentification, γ -conversion and π/K -decays in the electron sample, we use the following cuts:

- Momentum of the electron $p > 1.5$ GeV
- Aplanarity $A > 0.02$.

The aplanarity cut rejects very effectively the background contributions from light quarks.

Additional backgrounds result from a contamination of the multihadronic one photon annihilation sample with events from the following reactions:

(1) The deep inelastic electron-photon scattering (DIS)

$$e^+ e^- \rightarrow e^+ e^- + X (C = +).$$

* Parameters used at $W=34$ GeV: The mean transverse momentum $\sigma=0.30$ GeV/c, the relative abundance of u, d, s quarks from the sea 3:3:1, the relative proportion of pseudoscalar and vector mesons produced $P/(P+V)=0.55$, the fragmentation parameter in the Feynman-Field parameterization $AF=0.70$, the strong coupling constant $\alpha_s=0.19$

Here X is a hadronic system. One of the outgoing electrons is at large transverse momentum, the quasi-real target photon is emitted by the electron which is scattered at small angles and is not detected.

(2) The inelastic Compton scattering process (IC)

$$e^+ e^- \rightarrow e^+ e^- + X (C = -).$$

This can be considered as a radiative Bhabha process where a real photon is replaced by a massive one. This in turn converts to the hadronic system X .

The contributions of these two processes were computed according to methods applied in previous analyses [14, 15]. Events from DIS were generated using the structure function given in [16], which takes into account contributions from vector dominance, the quark-parton model and QCD corrections to the quark-parton model.

Events of these two reactions are very efficiently rejected by the selection criteria for multihadronic events and the aplanarity cut. To reduce this background further, we demand that the sum of the momenta of the charged particles in the same hemisphere (defined by the thrust axis) as the electron, projected onto the direction of this electron track, is larger than 1.0 GeV/c.

c) Signal of Prompt Electrons

The various contributions to the electron candidates with $p_{\perp} > 0.5$ GeV/c at $W = 14$ GeV and with $p_{\perp} > 1.0$ GeV/c at $W = 22$ and 34 GeV are shown in

Table 1. Contributions to the electron yield for electrons with $p > 1.5$ GeV, $p_{\perp} > 0.5$ GeV/c at $W = 14$, and $p_{\perp} > 1.0$ GeV/c at $W = 22$ and 34 GeV using $\text{Br}(c \rightarrow e\nu X) = 9\%$ and $\text{Br}(b \rightarrow e\nu X) = 12\%$

Source of electrons	$W = 14$ GeV	$W = 22$ GeV	$W = 34$ GeV
Light quarks (u, d, s)			
Misidentified π 's	5.9%	5.5%	7.6%
Converted photons, π/K decay	11.8%	2.8%	11.8%
IC	0.0%	0.2%	1.4%
DIS	1.3%	2.8%	3.5%
Heavy quarks (c, b)			
Misidentified π 's	4.2%	4.2%	8.0%
Converted photons, π/K decay	3.8%	4.4%	10.9%
Prompt electrons			
(all)	73.0%	80.1%	56.8%
$b \rightarrow e$ only	36.6%	60.0%	34.2%
Number of electron candidates	6	8	20

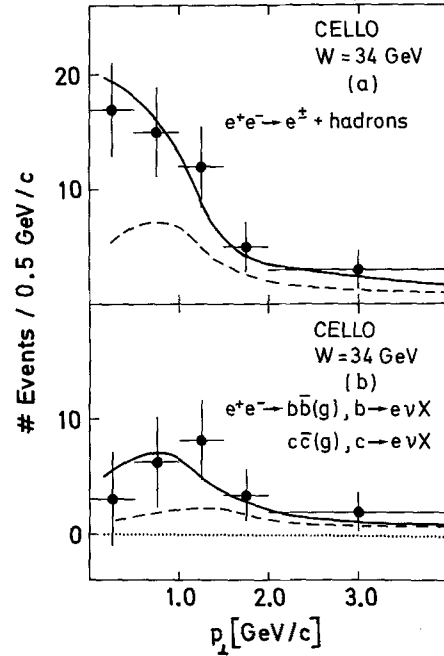


Fig. 1a and b. Distribution of the transverse momentum p_{\perp} for electrons compared to MC simulation with branching ratios of 12% for $b \rightarrow e\nu X$ and 9% for $c \rightarrow e\nu X$. **a** All electron candidates. The solid line shows the MC expected yield. The dashed line gives the contribution from prompt electrons as expected from MC events. **b** Prompt electrons. The solid line shows the prompt electron yield as expected from the MC events. The dashed line gives the MC expected contribution to the prompt electron yield resulting from the semileptonic decay $b \rightarrow e\nu X$

Table 1. Figure 1 shows the comparison between the data and the MC prediction for the p_{\perp} -spectrum of the electrons at the highest c.m. energy. The sample of electron candidates is displayed in Fig. 1a together with the total MC expected yield (solid line) and the MC expected prompt lepton yield (dashed line). A good agreement between data and MC is observed. The p_{\perp} -distribution of prompt electrons obtained after background subtraction is shown in Fig. 1b and compared to the MC expected prompt electron yield (solid line). The dashed line gives the contribution of the semileptonic b -decay only.

The systematic error of the electron yield is comprised of the relative systematic errors on the electron identification (10%), pion rejection (20%), detector simulation – in particular photon conversion (5%) and model dependence. The latter will be discussed in detail in Chap. V. The relative error on the model calculations for the DIS and IC processes is estimated to be 5%. Adding the various contributions quadratically we arrive at absolute systematic errors on the prompt electron yield of 6.9%, 8.3% and 7.7% respectively at the three c.m. energies.

IV. Prompt Muons

a) Muon Identification

Inclusive muon candidates are selected by using the information provided by the muon detector. To identify muons, space points reconstructed in the muon chambers are associated with the charged particles recorded by the central detector and extrapolated to the chambers. The uncertainties due to the track reconstruction in the central detector, multiple Coulomb scattering in the hadronic filter and distortions of the extrapolation through the magnetic field are taken into account. This yields for each extrapolated track an error σ in its position in the chamber plane. The association between hits and tracks is tested by two quantities: the distance d between predicted and measured hit, and the quality of association q , roughly equal to d/σ . The extrapolation procedure and the calculation of σ have been established using cosmic muons, and have been used in the μ -pair analysis [17].

For muon candidates a momentum greater than 1.6 GeV/c is required in order to have a probability of close to 100% to penetrate the hadron filter. We cut at $|\cos\theta| \leq 0.85$ in the polar angle to ensure a good momentum measurement of the muon. To associate hits in the muon chambers we demand $q \leq 3$ and $d \leq 40$ cm. These latter two cuts aim at reducing the hadronic background in the inclusive muon sample.

In addition the liquid argon calorimeter information is employed to reduce the hadronic background further. Noninteracting particles are enhanced by asking for an energy deposit of less than 500 MeV in the last two layers of the calorimeter (11–22 X_0).

b) Background Subtraction

There are two different background sources: Random associations between tracks and background hits in the muon chambers, π/K -decay and hadron punch-through. Random associations are suppressed by the d cut, whereas the q cut is more powerful in reducing the contamination from decay and punch-through. A detector simulator has been used to understand this contamination. It was tuned by comparing the results of the propagation of pions and protons through iron of different thicknesses with measurements [18]. The distribution of background hits in the muon chambers for Bhabha events was used to simulate the random associations. One can remark that mostly the randomly associated hadrons are sensitive to the liquid argon cut. The resulting hadron misidentification probabil-

Table 2. Contributions to the muon yield for muons with $p > 1.6$ GeV/c, $p_{\perp} > 0.5$ GeV/c at $W=14$ and $p_{\perp} > 1.0$ GeV/c at $W=22$ GeV and $W=34$ GeV using $\text{Br}(c \rightarrow \mu\nu X) = 9\%$ and $\text{Br}(b \rightarrow \mu\nu X) = 12\%$

Source of muons	$W=14$ GeV	$W=22$ GeV	$W=34$ GeV
π/K -decay	10%	9%	9%
hadron-punch through	18%	22%	22%
Random associations	3%	5%	14%
Prompt muons (all)	69%	64%	55%
$b \rightarrow \mu$ only	47%	40%	44%
Number of muon candidates	25	14	22

ity from π/K decay and hadron punch through is typically $5 \pm 1 \cdot 10^{-3}$ at 2 GeV and $12 \pm 2 \cdot 10^{-3}$ at 7 GeV.

The uncertainty in the background simulation is mainly due to punch through which is the dominating background source (see Table 2). The corresponding relative systematic error is estimated to be of the order of 10%.

c) Prompt Muon Signal

The selection criteria described above are used to obtain muon candidates. The result is shown in Table 2 where the different contributions to the total muon yield are listed. The MC generation of events was done using the Lund program* [6]. Figure 2a shows the transverse momentum of the muon candidates with respect to the thrust axis for the data at $W=34$ GeV and MC generated events (solid line). The dashed line shows the fraction of prompt muons expected from MC events. The corresponding distribution for the prompt muons as obtained after background subtraction is shown in Fig. 2b and compared to the MC expected yield (solid line). The dashed line gives the corresponding fraction of muons expected from the semileptonic b -decay.

The acceptance of our selection criteria has again been studied at the three c.m. energies using hadronic events. The main losses are due to the cut in the polar angle for the central detector acceptance (78%) and to the global muon detector acceptance and efficiency (80–85%, systematic error of 3%). The resulting acceptance for muons of momentum greater than 1.6 GeV/c is $55 \pm 5\%$ at $W=14$ GeV, $52 \pm 5\%$ at $W=22$ GeV, and $47 \pm 5\%$ at $W=34$ GeV. From these acceptances we derive a cross section for the production of prompt muons in multi-hadronic

* The parameters used at $W=34$ GeV [19]: $\sigma_q = 0.30$ GeV/c, $u:d:s = 3:3:1$, $P/(P+V) = 0.5$, $\alpha_s = 0.26$

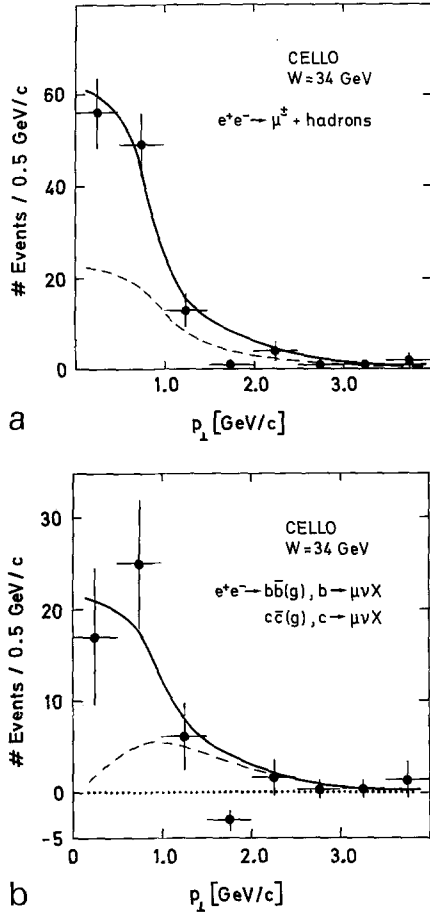


Fig. 2 a and b. Distribution of the transverse momentum p_{\perp} for muons compared to MC simulation with branching ratios of 12% for $b \rightarrow \mu\nu X$ and 9% for $c \rightarrow \mu\nu X$. **a** All muon candidates. The solid line shows the MC expected yield. The dashed line gives the contribution from prompt muons as expected from MC events. **b** Prompt muons. The solid line shows the prompt muon yield as expected from MC events. The dashed line gives the MC expected contribution to the prompt muon yield resulting from the semileptonic decay $b \rightarrow \mu\nu X$

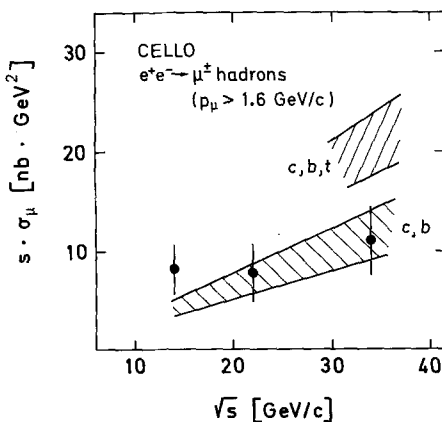


Fig. 3. Cross section of prompt muons with $p > 1.6 \text{ GeV}/c$ at the three c.m. energies, compared to MC expectations. The error bars include both statistical and systematic uncertainties

events. Figure 3 shows this cross section as a function of W , compared to the MC expectations for c and b production ($\text{Br}(c \rightarrow \mu) = 9 \pm 2\%$ and $\text{Br}(b \rightarrow \mu) = 12 \pm 2\%$). Effects due to different fragmentation functions (see Chap. V) are included in the band of expectations. The effect of adding a top quark with a muonic branching ratio of 12% is also indicated.

V. Influence of MC Event Generator and Fragmentation Schemes

Since the prompt lepton candidates are selected by kinematical and topological cuts, their expected yield will depend on the various assumptions made in the generation of multihadronic events. For this reason a detailed study was done to understand the systematic errors due to the choice of different MC generators, to the uncertainties on the fragmentation parameters and to different fragmentation functions. We report here the results obtained at 34 GeV with the Hoyer generator [5], followed by a comparison with the Lund one [6]. Results are quoted in terms of the lepton yield from c - and b -semileptonic decays normalized to 10,000 generated events. As throughout the paper the branching ratios were taken to be $\text{Br}(c \rightarrow l\nu X) = 9\%$ and $\text{Br}(b \rightarrow l\nu X) = 12\%$. An acceptance cut of $|\cos\theta| < 0.85$ was applied to each particle. An additional cut of $|\cos\theta| < 0.84$ was applied to the resulting thrust axis. Finally only leptons with a momentum larger than 1.6 GeV/c were considered. The relevant MC parameters have been varied one by one to understand their individual contribution to the total lepton yield.

a) Particle decay, QCD Matrix Element and α_s

Although the Hoyer MC can reproduce rather well the global features of the multihadronic events produced in e^+e^- [19], some of the details are not as well reproduced as needed for the determination of the semileptonic branching ratios of heavy quarks:

- The semileptonic decay of heavy mesons is performed in the program according to phase space. The universality of weak interactions and experimental data from charmed mesons suggest instead that a $(V-A)$ -decay matrix element is more adequate to reproduce the energy spectrum of leptons. This variation of the matrix element leads to a 23% decrease of the prompt lepton yield from c , but does not affect the yield from b significantly.

- The generator uses the 1st order massless-quark QCD matrix element [20] to evaluate the probability of gluon emission and the differential cross section for 3-jet production [21]. The 1st order QCD formula for heavy quarks leads to quark-mass de-

pendent probabilities of gluon emission [22]. However, introducing this mass-dependent matrix element, no appreciable effect on the lepton yield has been observed.

– A variation of the strong coupling constant α_s by as much as 20% does not change the prompt lepton yield considerably.

In summary we attribute systematic errors of 5% to c - and b -decays after normalizing to the $(V-A)$ -decay matrix element.

b) Fragmentation Parameters

Changing in the Hoyer MC the value of the fragmentation parameters σ_q , $u:d:s$ and $P/(P+V)$ within experimentally reasonable limits has shown that the prompt lepton yields from c and b are only very little affected.

The transverse momentum of a final state hadron depends on its rank in the fragmentation cascade. The first rank mesons have on average a smaller transverse momentum than the higher rank ones, because they get only one single contribution to p_\perp from sea quarks. Field and Feynman had suggested to give a random p_\perp also to the primary quark so that all mesons follow the same p_\perp distribution. We have tested the consequence of this hypothesis, giving uncorrelated transverse momenta to the original quarks. Also in this case no effect on the prompt lepton yield has been observed outside the statistical errors.

We estimate therefore that the overall systematic errors due to fragmentation parameters does not exceed 5%. Equivalent studies as described in a) and b) have been performed with the Lund MC and have given similar results.

c) Event Generators

Differences between the Hoyer and Lund generators were investigated. All parameters were set to identical values where possible. The yield from b -decays is not significantly different in the two models in contrast to the yield for the c -decay which is 18% lower in the Lund MC. The differences do not influence the yield from b -decays, but result in an 18% lower yield for the c -decay in the Lund MC. We thus estimate an overall systematic error of 18% for the c -decay and of 5% for the b -decay.

d) Fragmentation Functions for Heavy Quarks

In the previous part we have discussed the influence of various methods used in the MC generators. Here we discuss the important question of the description

of the fragmentation of the heavy quarks in terms of analytic functions $f(z)$, where z is the fractional longitudinal energy of the hadron in the fragmentation cascade. In the present analysis we apply a momentum cut on the lepton and are therefore sensitive to the choice of $f(z)$ which determines the momentum distribution. To understand the systematic effects we generated MC events using different forms of $f(z)$.

The standard MC generators [5–6] apply almost flat fragmentation functions for c and b quarks. Data available for the c -quark fragmentation [23] favour a much harder function $f(z)$ like those proposed in [24] and [25]. For the b -quark $f(z)$ is very poorly known, but is expected to be even harder than for the c -quark. We therefore tested the influence of the following functions:

- Flat: $f_c(z) = f_b(z) = 1$
- Lund: $f_q(z) = (1 + a_q)(1 - z)^{a_q}$
with $a_c = 0.216$ and $a_b = 0.086$,
- Peterson et al. [24]:

$$f_q(z) = \frac{1}{z \left(1 - \frac{1}{z} - \frac{\epsilon_q}{1-z}\right)^2}$$

with $\epsilon_c = 0.11$ and $\epsilon_b = 0.013$,

- Suzuki et al. [25]:

$$f(z) = \exp\left(-\frac{1}{2m_\pi}(m_q + M)\left(z + \frac{\alpha_q}{z}\right)\right), \quad z > \alpha_q$$

$$\text{with } M = 1 \text{ GeV}, \quad \alpha_q = \left(\frac{m_M}{m_q + M}\right)^2.$$

$$f(z) = 0, \quad z < \alpha_q$$

These functions were introduced both into the Hoyer and the Lund generator without retuning the MC parameters. The relative changes are quite similar. We therefore present the results from the Lund generator only. Table 3 shows the number of prompt leptons expected from c and b decays for 10,000 gen-

Table 3. Influence of different fragmentation functions $f(z)$ in the Lund M.C. event generator on the number of leptons (muons or electrons) with $p > 1.6$ GeV/c for 10,000 multihadronic events at $W = 34$ GeV using $\text{Br}(c \rightarrow l\nu X) = 9\%$ and $\text{Br}(b \rightarrow l\nu X) = 12\%$

$f(z)$	No p_\perp -cut		$p_\perp > 1$ GeV/c	
	$c \rightarrow l\nu X$	$b \rightarrow l\nu X$	$c \rightarrow l\nu X$	$b \rightarrow l\nu X$
Flat	160.0 ± 4.0	92.2 ± 3.0	19.5 ± 1.4	62.9 ± 2.5
Lund	154.4 ± 3.9	94.6 ± 3.1	20.2 ± 1.4	64.8 ± 2.5
Peterson et al.	208.5 ± 4.6	101.9 ± 3.2	27.2 ± 1.6	67.9 ± 2.6
Suzuki	225.3 ± 4.7	109.9 ± 3.3	33.7 ± 1.8	73.0 ± 2.7

erated multihadronic events for the four different functions. These events were subjected to the same cuts as in the preceding paragraphs. The lepton yields are shown with and without a p_{\perp} -cut at 1 GeV/c separately after the p -cut at 1.6 GeV/c.

We observe large differences between soft and hard functions with and without the p_{\perp} -cut. Even between the two more realistic hard $f(z)$ we observe differences in the order of 15% for the c -decay in contrast to the b -decay (5%) which is much less sensitive. Therefore a systematic error in the determination of the branching ratio of the semileptonic decay is introduced not only for the c -quark, but also for the b -quark due to the subtraction of the c -quark contribution.

In summary applying the Peterson et al. fragmentation function and the $(V-A)$ -decay matrix element we estimate an overall relative systematic error due to all MC dependent effects of 25% for c -decays and 10% for b -decays.

VI. Results

We derive from the prompt leptons the branching ratios of the semileptonic decay of the c - and b -quark by comparing the p_{\perp} spectra of the data with the MC prediction of fixed branching ratios.

As discussed previously the leptons from b -decays are expected to have high transverse momenta. To enrich the b -sample we therefore take events with $p_{\perp} > 0.5$ GeV/c at $W=14$ and with $p_{\perp} > 1.0$ GeV/c at $W=22$ and $W=34$ GeV. With these cuts the accepted fractions of events with a semileptonic b -decay is 37%, 60%, 34% for the electron decay and 47%, 40%, 44% for the muon decay at $W=14$, 22 and 34 GeV. Table 4 shows the derived branching ratios using the fragmentation functions of [24] and $(V-A)$ -decay. The branching ratio of $c \rightarrow l\nu X$ was taken as $9 \pm 2\%$. The systematic errors include those discussed in the lepton identification and background subtraction and those due to the fragmentation and methods specific to the MC event generation (Table 3). They were added in quadrature. We

Table 4. Branching ratios for the semileptonic decay of the heavy quarks at three c.m. energies W . The first error is the statistical one, the second error the systematic one

W (GeV)	Branching ratios		
	$b \rightarrow e\nu X$	$b \rightarrow \mu\nu X$	$c \rightarrow \mu\nu X$
14	$4.0 \pm 11.0 \pm 4.3\%$	$26.0 \pm 8.2 \pm 3.9\%$	$20.5 \pm 7.2 \pm 4.9\%$
22	$21.3 \pm 10.5 \pm 2.1\%$	$3.8 \pm 6.2 \pm 3.7\%$	$15.0 \pm 4.9 \pm 3.4\%$
34	$15.5 \pm 9.0 \pm 2.8\%$	$6.3 \pm 4.8 \pm 3.5\%$	$8.1 \pm 4.3 \pm 3.9\%$
Average	$14.1 \pm 5.8 \pm 3.0\%$	$8.8 \pm 3.4 \pm 3.5\%$	$12.3 \pm 2.9 \pm 3.9\%$

Table 5. Comparison of branching ratios for the semileptonic decay of the heavy quarks from this experiment to those of other experiments

	Branching ratios		
	$b \rightarrow e\nu X$	$b \rightarrow \mu\nu X$	$c \rightarrow \mu\nu X$
CELLO (this paper)	$14.1 \pm 5.8 \pm 3.0\%$	$8.8 \pm 3.4 \pm 3.5\%$	$12.3 \pm 2.9 \pm 3.9\%$
CLEO [3]	$12.7 \pm 1.7 \pm 1.3\%$	$12.2 \pm 1.7 \pm 3.1\%$	
CUSB [3]	$13.6 \pm 2.5 \pm 3.0\%$		
Mark-J [3]		$10.5 \pm 1.5 \pm 1.3\%$	$11.5 \pm 1.0 \pm 1.7\%$

find an average branching ratio of 14.1 ± 5.8 (stat.) ± 3.0 (syst.)% for $b \rightarrow e\nu X$ and of 8.8 ± 3.4 (stat.) ± 3.5 (syst.)% for $b \rightarrow \mu\nu X$, in good agreement with previous results [3] (see Table 5).

To extract the branching ratios for the semileptonic decay of c -quarks we use cuts in the thrust distribution of $T > 0.88$, 0.88 and 0.94 at the three c.m. energies ($W=14$, 22 and 34 GeV). Due to large contributions from background processes to the electron signal we are only able to determine the muonic branching ratio. With these cuts the accepted fractions of events containing a muon from semileptonic c -decay are 43%, 43%, 34% at the three c.m. energies with negligible contributions from b -decay. Column 3 in Table 4 contains the $c \rightarrow \mu\nu X$ branching ratios with an average of 12.3 ± 2.9 (stat.) ± 3.9 (syst.)% again in agreement with previous measurements [4] (see Table 5).

Replacing the relatively hard fragmentation functions of [24] by the standard functions of the Hoyer and Lund generators would increase the branching ratios by 16% for $b \rightarrow e\nu X$, by 29% for $b \rightarrow \mu\nu X$ and by 36% for $c \rightarrow \mu\nu X$.

We have searched for events with 2 leptons and found e.g. at $W=34$ GeV $1ee$, $5\mu\mu$ and $2e\mu$ candidates. Within the limited statistics these numbers are compatible with the expectations from MC using the measured branching ratios of the c - and b -quark.

Using the sample of enriched $b\bar{b}$ -events, we determined the asymmetry due to the electro-weak interference. We use the thrust axis as an approximate measurement of the quark direction of flight and the sign of the lepton to tag the charge of the parent quark. After background subtraction we fit the angular distribution of the asymmetry. For $b\bar{b}$ -pair production an asymmetry of -27.3% is predicted. Due to the various background contributions we expect a reduced asymmetry of -5.8% for electrons and -8.0% for muons at $W=34$ GeV with an uncertainty of 2.2% for electrons and 3.2% for muons respectively. This error on the predicted value in-

cludes all systematic uncertainties discussed above: lepton identification, model dependence and branching ratios. Even though we cannot really test in a definitive way these predictions with our limited statistics, our measurements of $-38\% \pm 21\%$ for electrons and of $-43\% \pm 31\%$ for muons are compatible with the expected values.

Acknowledgement. We are indebted to the PETRA machine group and the DESY computer center for their excellent support during the experiments. We acknowledge the invaluable effort of all engineers and technicians of the collaborating institutions in the construction and maintenance of the apparatus, in particular the operation of the magnet system by G. Mayaux and Dr. Horlitz and their groups. The visiting groups wish to thank the DESY directorate for the support and kind hospitality extended to them. This work was partly supported by the Bundesministerium für Forschung and Technologie.

References

1. M. Kobayashi, T. Maskawa: Prog. Theor. Phys. **49**, 652 (1973)
2. Xuan Yen Pham: Proc. XVIIth Rencontre de Moriond, 83 (1982); L. Montanet: *ibid.*, 45
3. For a recent review G. Kalmus: Rapporteur's talk at the XXI. International Conference on High Energy Physics, Paris, July 1982, RL-82-090 (1982); CLEO Collab. K. Chadwick et al.: Phys. Rev. **D27**, 475 (1983); CUSB Collab. L.J. Spencer et al.: Phys. Rev. Lett. **47**, 771 (1981); MARK-J Collab. B. Adeva et al.: DESY-83-029 (1983)
4. For a recent review G.H. Trilling: Phys. Rep. **75**, 57 (1981); W. Bacino et al.: Phys. Rev. Lett. **40**, 671 (1978); Phys. Rev. Lett. **43**, 1073 (1979); Phys. Rev. Lett. **45**, 329 (1980); J.M. Feller et al.: Phys. Rev. Lett. **40**, 274 (1978); R.H. Schindler et al.: Phys. Rev. **D24**, 78 (1981); MARK-J Collab. B. Adeva et al.: DESY-83-029 (1983)
5. Hoyer et al.: Nucl. Phys. **B161**, 349 (1979)
6. B. Anderson et al.: Phys. Lett. **94B**, 211 (1980)
7. J. Jersak et al.: Phys. Lett. **98B**, 363 (1981); M.J. Puhala et al.: Phys. Rev. **D23**, 89 (1981)
8. CELLO Collab. H.J. Behrend et al.: Phys. Scr. **23**, 610 (1981)
9. CELLO Collab. H.J. Behrend et al.: DESY Rep. 81-029 (1981)
10. R.L. Ford, W.R. Nelson: EGS Code, SLAC Rep. 210 (1978)
11. RSIC Computer Code Collection: HETC Code, Oak Ridge National Laboratory, CCC-178
12. CELLO Collab. H.J. Behrend et al.: Z. Phys. C - Particles and Fields **14**, 189 (1982)
13. R.D. Field, R.P. Feynman: Phys. Rev. **D15**, 2590 (1977); Nucl. Phys. **B136**, 1 (1978)
14. CELLO Collab. H.J. Behrend et al.: Phys. Lett. **118B**, 211 (1982)
15. CELLO Collab. H.J. Behrend et al.: DESY Rep. 83-018 (1983), to be published in Phys. Lett. B
16. C. Peterson et al.: Nucl. Phys. **B174**, 424 (1980)
17. CELLO Collab., H.J. Behrend et al.: Z. Phys. C - Particles and Fields **14**, 283 (1982)
18. H.G. Sander: Thesis RWTH Aachen Report HEP 74-07 (1974)
19. CELLO Collab. H.J. Behrend et al.: DESY Rep. 82-061 (1982), to be published in Nucl. Phys. B
20. J. Ellis et al.: Nucl. Phys. **B111**, 253 (1976); Erratum: Nucl. Phys. **B130**, 516 (1977)
21. G. Kramer et al.: Phys. Lett. **79B**, 249 (1978); Erratum: Phys. Lett. **80B**, 433 (1979)
22. G. Kramer et al.: Z. Phys. C - Particles and Fields **4**, 149 (1980)
23. K. Kleinknecht, B. Renk: UNIDO-82/274 (1982) The following data were used for their fit: CDHS Collab. J. Knobloch et al.: Proc. of the 9th Int. Conf. on Neutrino Physics and Astrophysics, Maui, Hawaii 1981, Vol. I p. 421; H. Abramowicz et al.: Z. Phys. C - Particles and Fields **15**, 19 (1982); Canada-Japan-Korea-USA Emulsion Collab. E 531, N. Ushida, et al.: Characteristics of Charmed Hadrons Produced by Neutrino Interactions, 10th Int. Conf. on Neutrino Physics and Astrophysics, Balatonfured, June 13-20, 1982, and Preprint McGill (Oct. 1982); MARK II Collab. J.N. Yelton et al.: Phys. Rev. Lett. **49**, 430 (1982); TASSO Collab.: talk by G. Wolf at 21st Conf. on High Energy Physics, Paris, July 26-31, 1982; CLEO Collab. C. Bebek et al.: Inclusive Charged D^* Production in e^+e^- Annihilations at $W=10.4$ GeV, CLEO 82-01, contribution to 21st Conf. on High Energy Physics, Paris, July 26-31, 1982
24. C. Peterson et al.: SLAC-PUB-2912 (1982); Phys. Rev. **D27**, 105 (1983)
25. M. Suzuki: Phys. Lett. **71B**, 139 (1977)